Angewandte Chemie
Eine Zeitschrift der Gesellschaft Deutscher Chemiker

Supporting Information

Controllable Encapsulation of "Clean" Metal Clusters within MOFs through Kinetic Modulation: Towards Advanced Heterogeneous Nanocatalysts

Hongli Liu, Lina Chang, Cuihua Bai, Liyu Chen, Rafael Luque, and Yingwei Li**

anie_201511009_sm_miscellaneous_information.pdf

Experimental Section

1. Catalyst preparation

All chemical reagents were purchased from commercial sources and used without further purification.

1.1 Synthesis of Pt@UiO-66

In a typical synthesis, 100 mg H_2BDC, 133.6 mg $ZrCl_4$, 9.5 mg $H_2PtCl_6 \cdot 6H_2O$, and the required amount of acetic acid were dissolved in 40 mL of DMF in a 100 mL tube under H_2/Air. The tube was sealed and the mixture was subjected to ultrasounication (180 Watt) for 0.5 h, and then stirred at 120 ºC for 24 h. After the slurry was cooled to room temperature, the solid was isolated by centrifugation, washed with DMF to remove the unreacted precursors. The resulting powder was dispersed in 50 mL of ethanol and subjected to sonication (40% energy efficiency) for 2 min, and then soaked for 8 h. The solvent exchange with ethanol was repeated five times. Finally, the solid was dried under vacuum (≤ 0.1 Pa) at 150 °C overnight.

1.2 Synthesis of Pt/UiO-66 by impregnation

UiO-66 was synthesized according to the reported procedures.[1] For supporting Pt NPs on the pre-synthesized UiO-66, 100 mg of activated UiO-66 was dispersed in 10 mL *N*,*N*-Dimethylformamide solution of H_2PtCl_6. Subsequently, the slurry was subjected to ultrasounication (180 Watt) for 10 min and was then magnetically agitated at 120 ºC for 24 h. Afterward, the solid was isolated by centrifugation, followed by washing thoroughly with DMF and solvent exchange with ethanol for five times. The as-synthesized sample was dried under vacuum (≤ 0.1 Pa) at 100 °C overnight to obtain the Pt/UiO-66.

1.3 Synthesis of Pt@UiO-66-PVP

100 mg H_2BDC, 133.6 mg $ZrCl_4$, acetic acid (120 equiv. to Zr), 9.5 mg $H_2PtCl_6 \cdot 6H_2O$, and PVP (5 equiv. to Pt) were dissolved in 40 mL of DMF in a 100 mL tube under H_2/Air with a volume ratio of 1:1. The tube was sealed and the mixture was subjected to ultrasounication (180 Watt) for 0.5 h, and then stirred at 120 ºC for 24 h. After the slurry was cooled to room temperature, the solid was isolated by centrifugation, washed with DMF. The resulting powder was dispersed in 50 mL of ethanol and subjected to sonication (40% energy efficiency) for 2 min, and then soaked for 8 h. The solvent exchange with ethanol was repeated for five times. Finally, the solid was dried under vacuum (≤ 0.1 Pa) at 150 °C overnight.

2. Catalyst characterization

Powder X-ray diffraction patterns of the samples were obtained on a Rigaku diffractometer (D/MAX-IIIA, 3 kW) using Cu Kα radiation (40 kV, 30 mA, 0.1543 nm).

The nitrogen adsorption-desorption isotherms were measured at 77 K on a Micromeritics ASAP 2020 instrument. Before the analysis, the samples were evacuated at 150 ºC for 12 h. The metal contents of the samples were determined quantitatively by atomic absorption spectroscopy (AAS) on a HITACHI Z-2300 instrument.

UV-visible spectroscopy was carried out using an UV-2450 spectrophotometer (Shimadzu, Japan). All spectra were background corrected using a spectrum obtained from the according mixture of DMF and acetic acid.

The size and morphology of the samples were investigated by using a transmission electron microscope (TEM, JEOL, JEM-2100F) with EDX analysis (Bruker XFlash 5030T) operated at 200 kV. Samples were suspended in ethanol and deposited straight away on a copper grid prior to analysis.

Pt dispersion of the catalysts was determined by CO pulse chemisorption measurement with a Micromeritics AutoChem II 2920 apparatus. Before analysis, the sample was treated at 200 °C in H_2 for 1 h. The dispersion, *D*, defined as the fraction of palladium at the surface, $D = Pt_s/Pt_{total}$, was calculated with the assumption of one CO molecule per surface Pt.[2]

3. Catalytic reactions

3.1 Liquid-phase hydrogenation of olefins

Olefin (0.1 mmol) and supported palladium catalyst (0.2 mol%) were added to 2 mL of THF. The reaction mixture was stirred at room temperature under 1 atm hydrogen atmosphere for 1 h. Upon reaction completion, the catalyst particles were removed from the solution by filtration and washed with THF. The liquid phase was subsequently analyzed by GC/MS (Agilent 7890B/5977A equipped with a 0.25 mm × 30 m DB-WAX capillary column).

3.2 Liquid-phase aerobic oxidation of alcohols

Typically, alcohol (0.5 mmol) and the catalyst (1 mol% Pt) were added to 5 mL of toluene. The reaction mixture was stirred at 80 ºC under 1 atm of O_2. Upon reaction completion, the catalyst particles were removed from the solution by filtration. The liquid phase was subsequently analyzed by GC/MS (Agilent 7890B/5977A equipped with a 0.25 mm × 30 m DB-WAX capillary column).

3.3 Reusability of the Pt@UiO-66 catalyst

For the recyclability tests, the reactions were performed under the same reaction conditions as described above, except using the recovered catalyst. Each time, the catalyst was separated from the reaction mixture by centrifugation at the end of catalytic reaction, thoroughly washed with toluene, and then heated at 150 ºC under vacuum.

Table S1 Characterization results of Pt@UiO-66 catalysts by CO pulse chemisorption.

Entry	Sample	Pt dispersion (%)
1	Pt@UiO-66 prepared under H_2/Air = 0:1	53.5
2	Pt@UiO-66 prepared under H_2/Air = 1:2	68.3
3	Pt@UiO-66 prepared under H_2/Air = 1:1	71.1
4	Pt@UiO-66 prepared under H_2/Air = 2:1	71.7
5	Pt@UiO-66-PVP	47.3
6	Pt/UiO-66	28.0

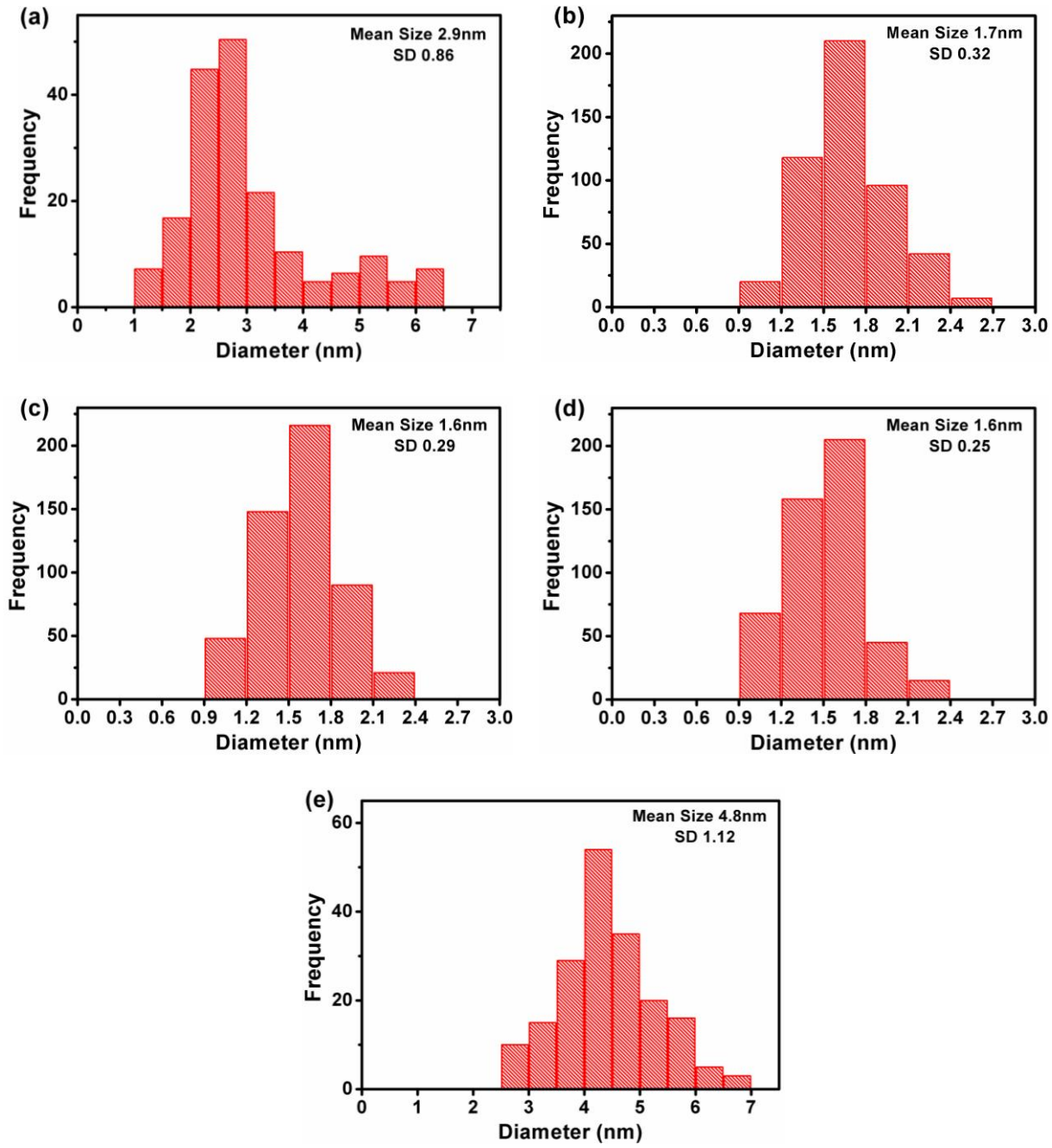

Figure S1. The corresponding size distribution histograms of Pt@UiO-66 nanocomposites prepared in the presence of H_2/Air with a volume ratio of 0:1 (a), 1:2 (b), 1:1 (c), and 2:1 (d), respectively; and Pt/UiO-66 (e).

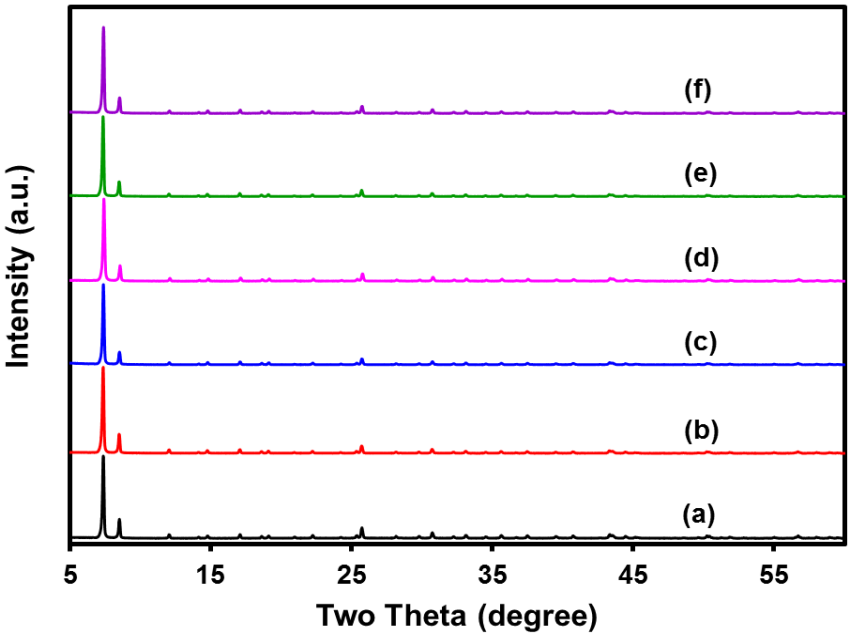

Figure S2. Powder XRD patterns of UiO-66 (a), and Pt@UiO-66 nanocomposites prepared in the presence of H_2/Air with a volume ratio of 0:1 (b), 1:2 (c), 1:1 (d), and 2:1 (e), respectively. The sample synthesized under H_2/Air volume ratio of 1:1 after catalytic reaction (f).

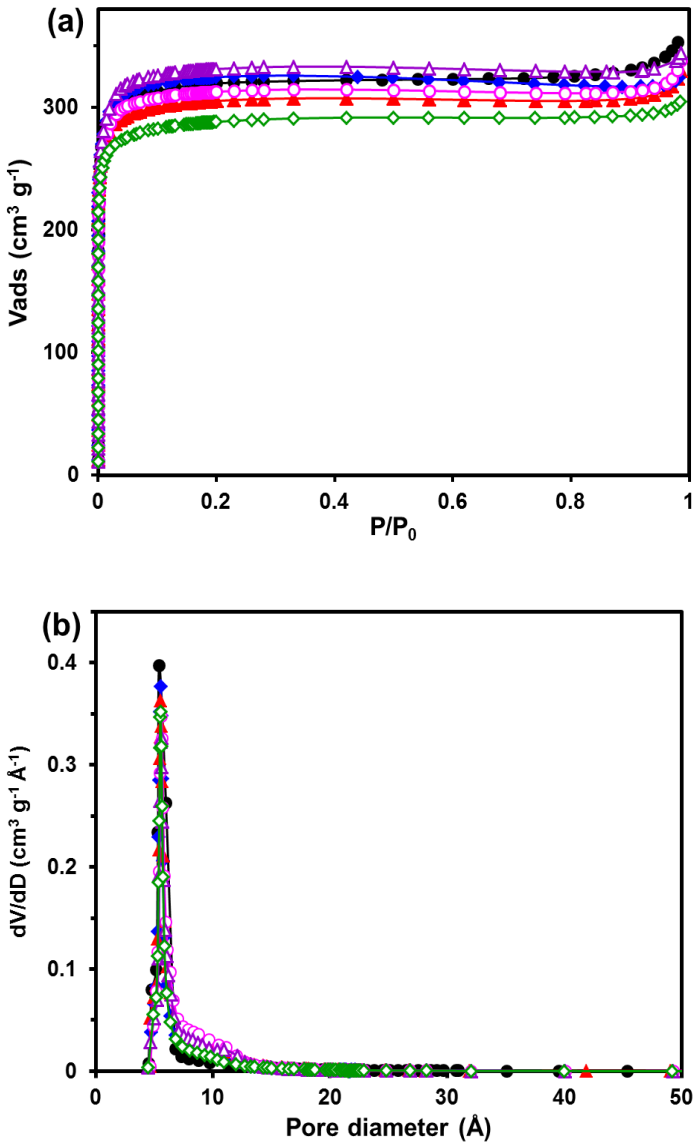

Figure S3. Nitrogen adsorption isotherms (a) and pore-size distribution curves (b) of UiO-66 (●), and Pt@UiO-66 nanocomposites prepared under H_2/Air with a volume ratio of 0:1 (◆), 1:2 (▲), 1:1 (○), and 2:1 (Δ), respectively. The sample synthesized under H_2/Air volume ratio of 1:1 after catalytic reaction (◇).

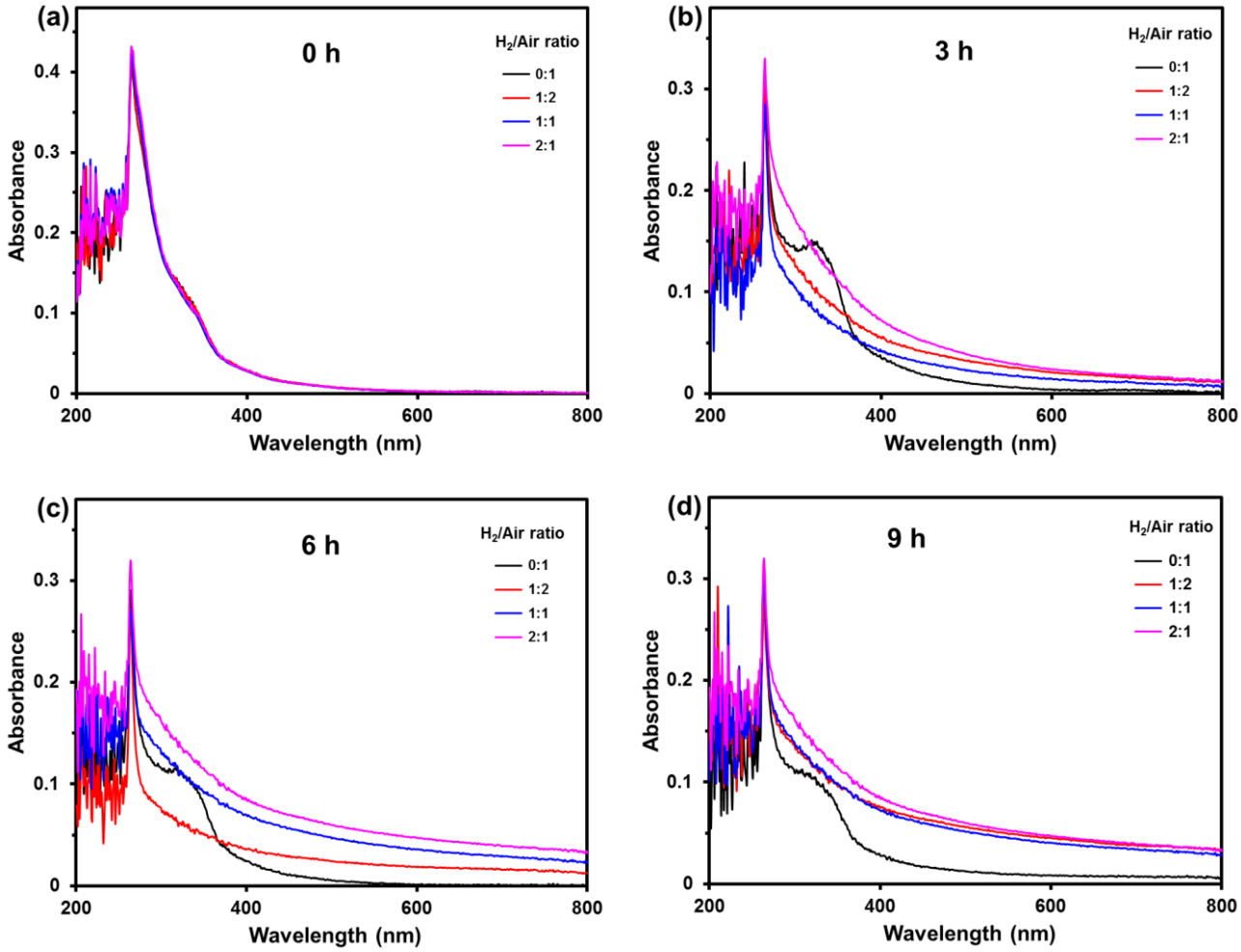

Figure S4. Time-resolved UV-vis absorbance spectra of H_2PtCl_6 in the mixed solution of DMF and acetic acid at 120 ºC under H_2/Air with a volume ratio of 0:1, 1:2, 1:1, and 2:1, respectively.

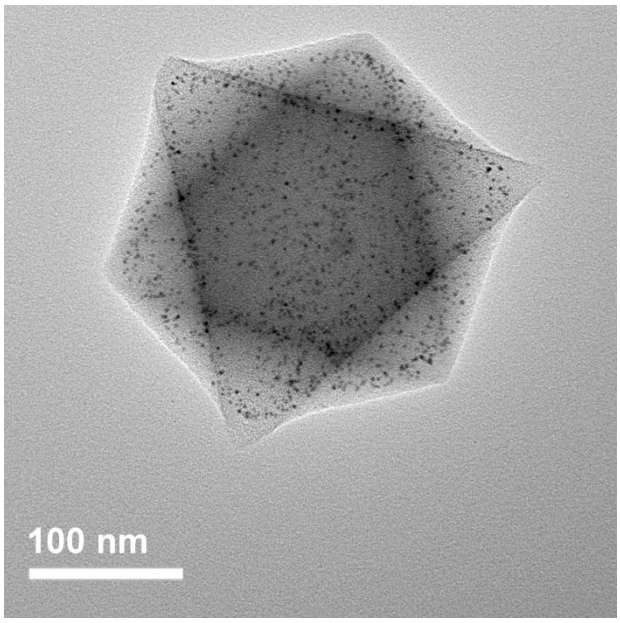

Figure S5. TEM image of the Pt@UiO-66 nanocomposite prepared in the presence of 0.2 equiv. dimethylamine to Pt under H_2/Air with a volume ratio of 1:1.

To further investigate the effect of the amine, we added dimethylamine (2.0 mol/L in THF, 0.2 equiv. to Pt) to the reaction mixture for Pt@UiO-66. The addition of dimethylamine did not affect the size and morphology of the sample as compared to Pt@UiO-66 (Figure 1c), which indicates that trace amounts of dimethylamine do not significantly influence the preparation of Pt@UiO-66.

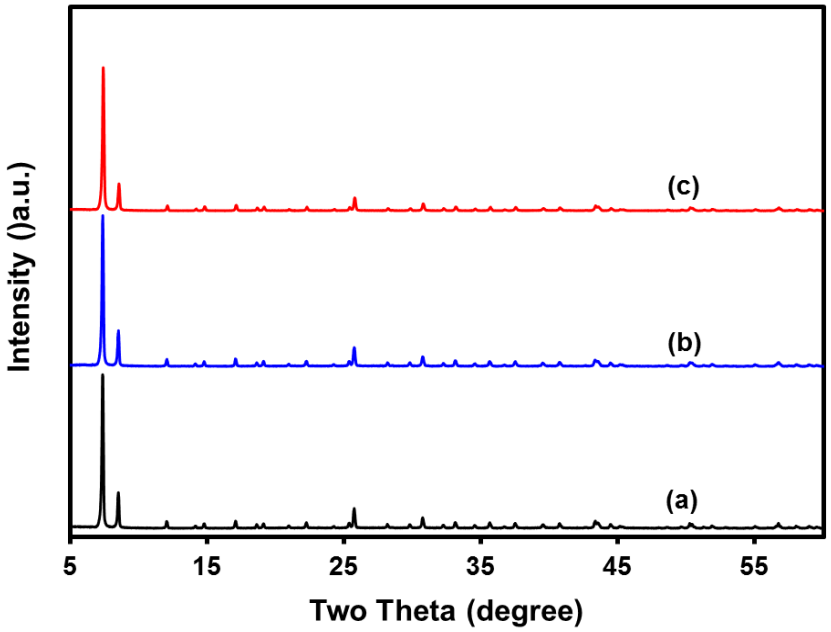

Figure S6. Powder XRD patterns of UiO-66 (a), and Pt/UiO-66 before (b) and after catalytic reaction (c).

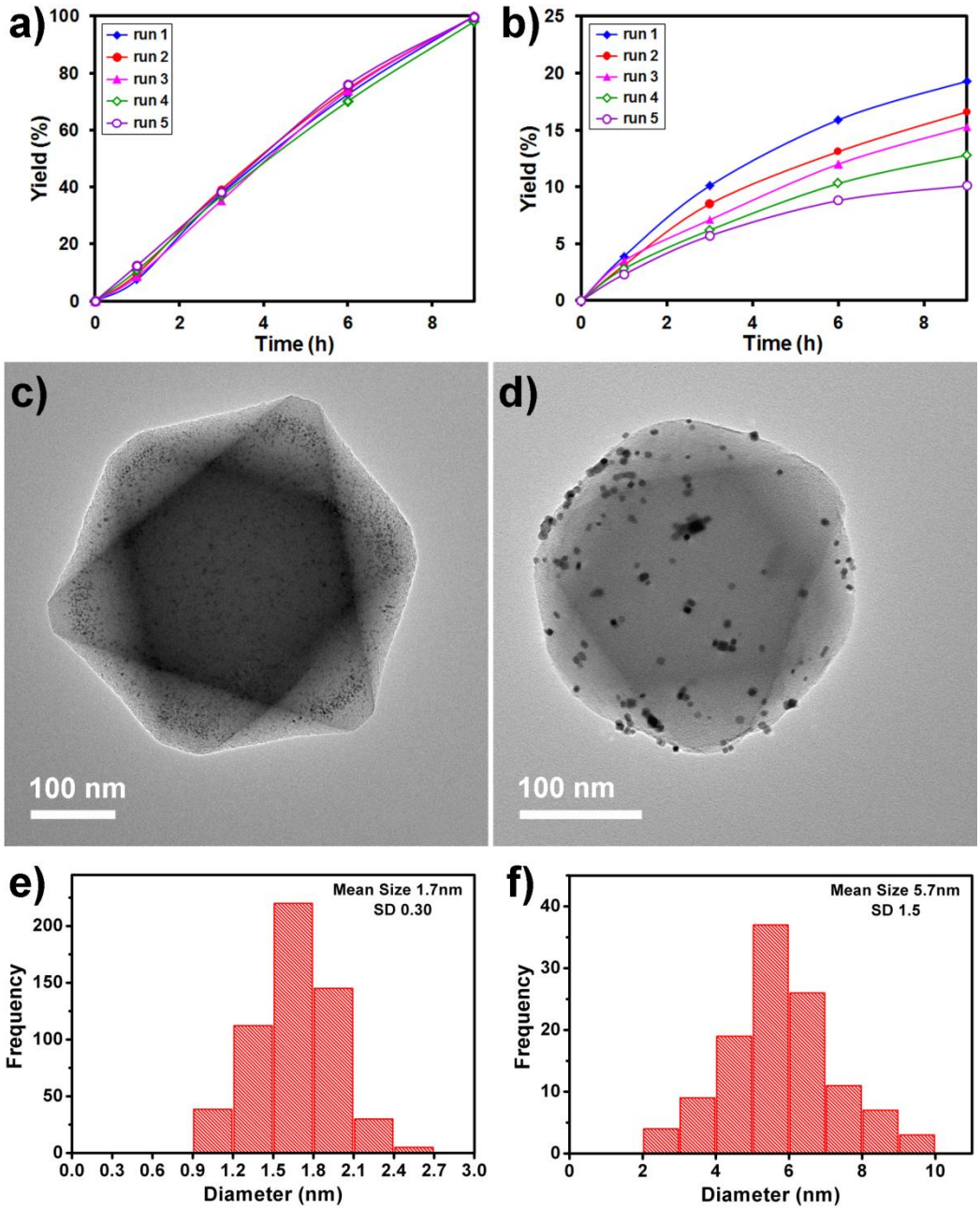

Figure S7. Reusability of the Pt@UiO-66 prepared under 1:1 H_2/Air (a), and Pt/UiO-66 (b) in the oxidation of cinnamyl alcohol. TEM images and corresponding particle size distribution histograms of the recycled Pt@UiO-66 (c, e) and Pt/UiO-66 (d, f) after being used for five times.

Heterogeneity test was performed to ascertain whether there was any homogeneous active species leached in reaction solution that could catalyse the oxidation. When the reaction proceeded at ca. 20% conversion, the catalyst was quickly removed by centrifugation and the isolated solution was further reacted for an additional 7 h (Figure S8). No further conversion of cinnamyl alcohol was observed under similar reaction conditions. Meanwhile, no metal traces were detected in the solution by AAS analysis.

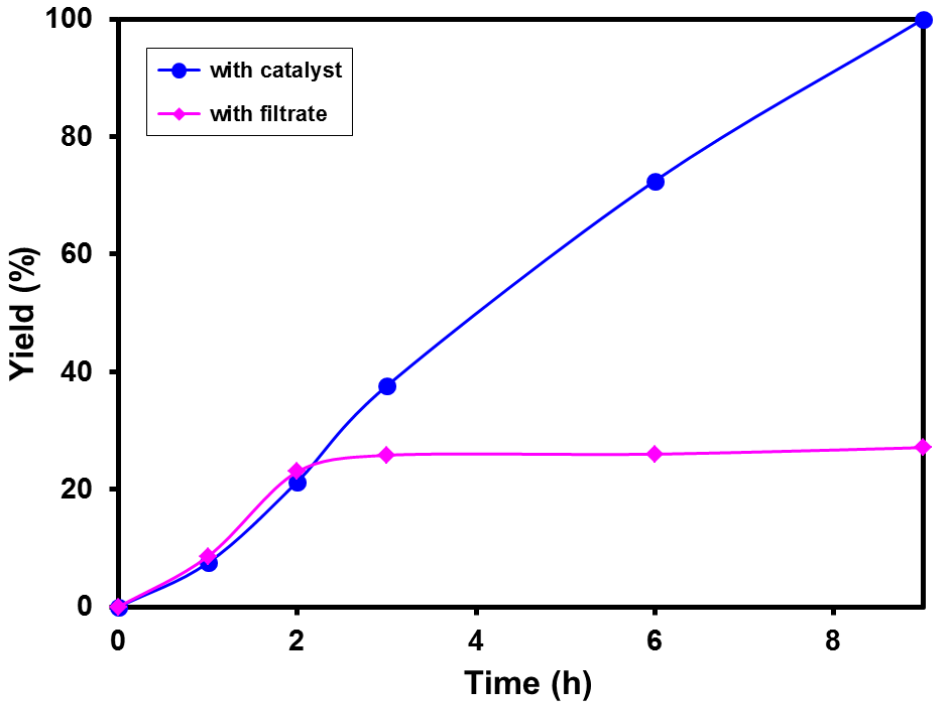

Figure S8. Activity profile for the aerobic oxidation of cinnamyl alcohol.

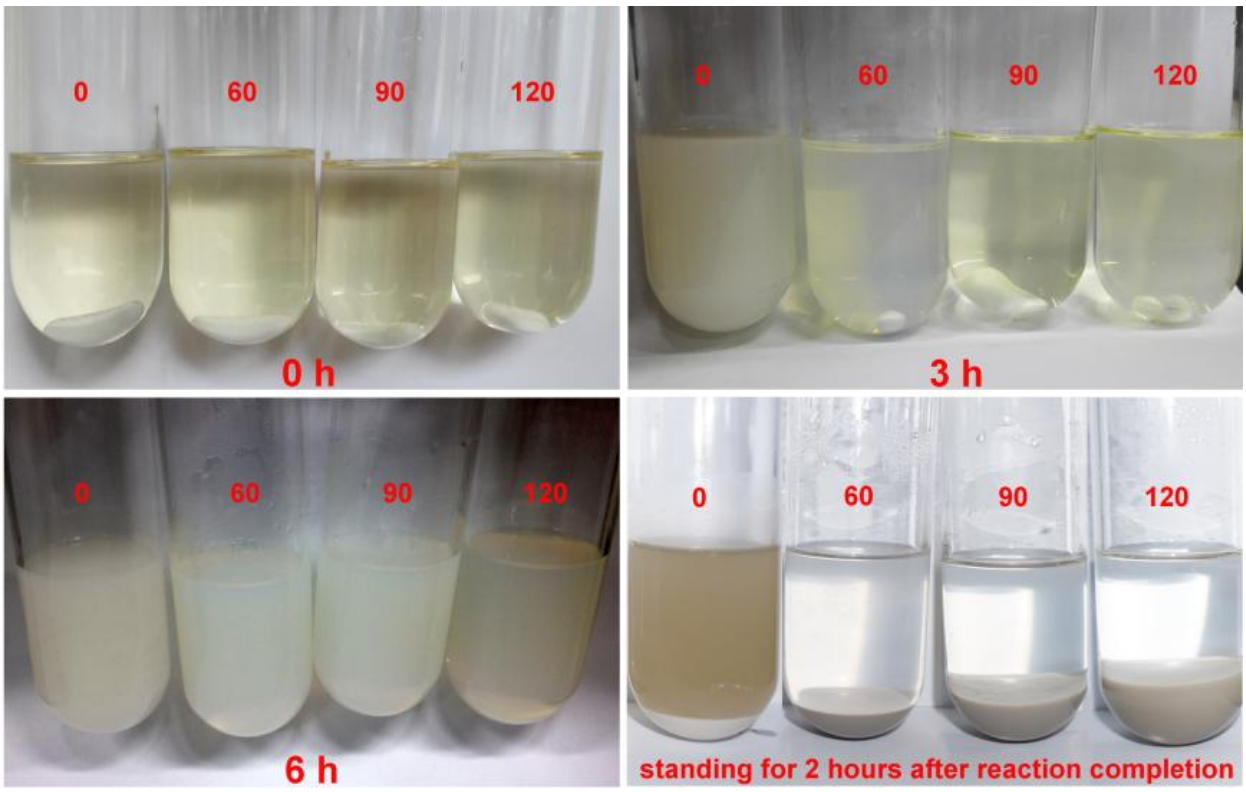

Figure S9. Time-evolution color changes of the reaction mixture for monitoring the formation of Pt@UiO-66 nanocomposites in the presence of different amounts of acetic acid (0, 60, 90, and 120 equiv. to Zr, respectively).

Synthesis conditions: 100 mg H_2BDC, 133.6 mg $ZrCl_4$, 9.5 mg $H_2PtCl_6 \cdot 6H_2O$ and the required amount of acetic acid (0, 60, 90, and 120 equiv. to Zr, respectively) were dissolved in 40 mL of DMF in a 100 mL tube under H_2/Air with a volume ratio of 1:1. The tube was sealed and the mixture was subjected to ultrasounication (180 Watt) for 0.5 h, and then stirred at 120 ºC.

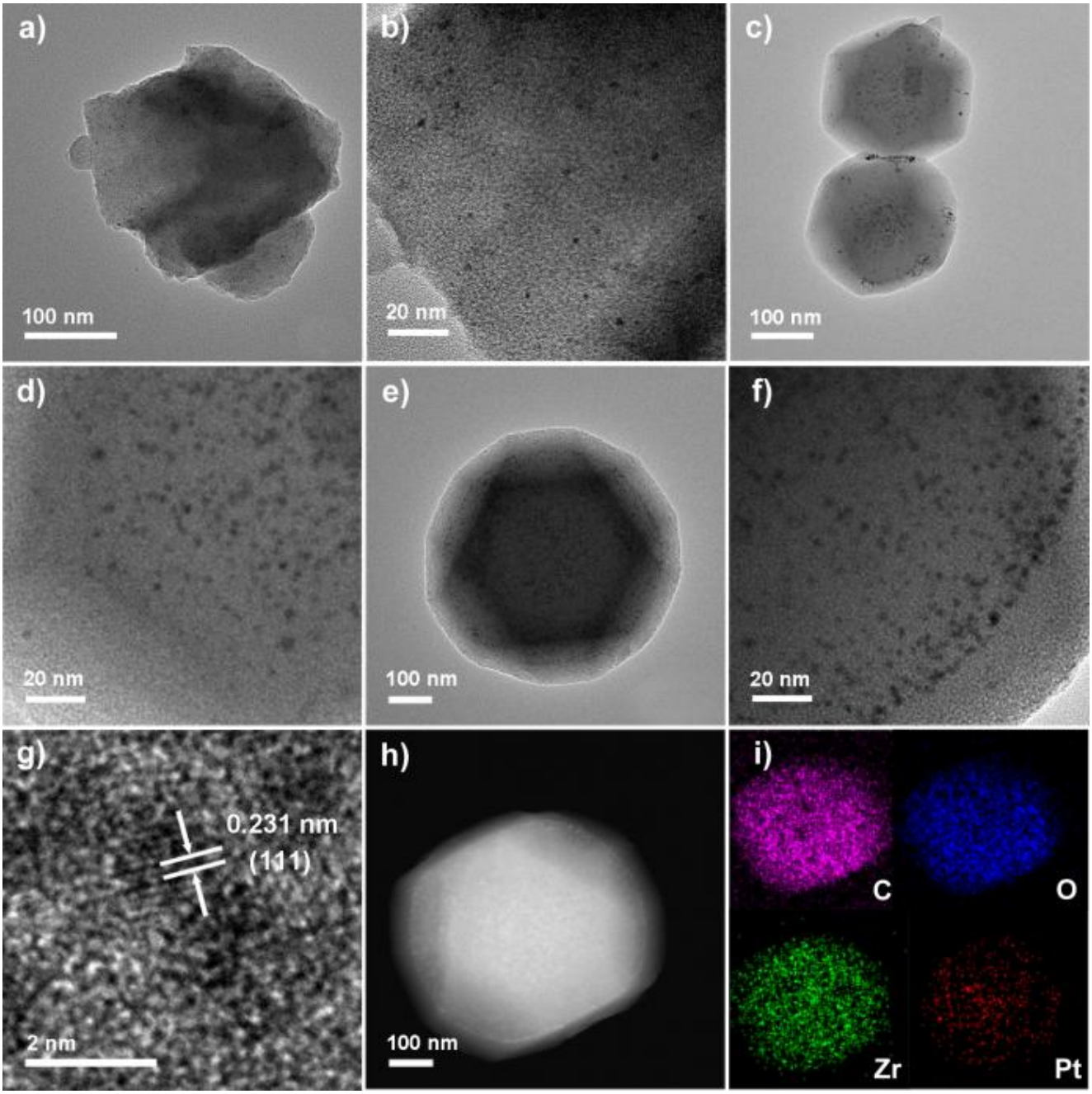

Figure S10. TEM images of Pt@UiO-66 nanocomposites prepared in the presence of 0 (a, b), 60 (c, d), and 90 (e, f, g) equivalents of acetic acid, respectively. HAADF-STEM image of Pt@UiO-66 prepared with 90 equiv. of acetic acid (h) and the corresponding EDX elemental mapping (i).

Inspired by the attractive properties, we attempted to extend the surfactant-free controlled encapsulation strategy to MOF-encapsulated metal materials by modulating the nucleation rate of MOF. It has been documented that acetic acid may act as modulator to regulate the nucleation and growth rate of MOFs.[3] Considering that the controlled encapsulation process was able to proceed in the presence of a significant amount of COO^- groups (on the linker terephthalic acid), we speculated the addition of acetic acid (only with COO^- group) would not

deteriorate the intrinsic interface between the MOF precursors and Pt clusters. Thus, the possibility of controlled incorporation of Pt clusters inside MOF was also examined by regulating the amount of acetic acid added in the synthesis.

The material preparation was performed in a DMF solution of $ZrCl_4$, 1,4-benzene dicarboxylic acid, and various amounts of acetic acid (0, 60, 90, and 120 equiv. to Zr) at 120 °C under 1:1 H_2/Air. The synthesis process can be visually monitored by the evolution of the reaction mixtures. As shown in Figure S9, the solution color was changed from transparent pale yellow to turbid fine white within 3 h in the absence of acetic acid, but was still transparent in the present of acetic acid. With an increase in acetic acid content, a distinctly longer time was needed for observing this change. These observations indicated that the formation rate of UiO-66 was slowed down with an increase in acetic acid amount, in good agreement with the previous reports.[3a,3b]

The structure and morphology of as-synthesized materials were analyzed by TEM. As can be seen in Figure S10a and S10b, Pt clusters with an average size of 1.4 ± 0.3 nm were highly dispersed on the UiO-66. When 60 equiv. of acetic acid was used, Pt clusters were evidently encapsulated within MOF crystals even with a little aggregation (Figure S10c, S10d). The crystallinity of UiO-66 was considerably improved and isolated MOF particles could be seen. More interestingly, upon further increasing the amount of acetic acid, Pt clusters with an average size of 1.8 ± 0.3 nm were homogeneously dispersed in UiO-66 and no significant aggregation was observed (Figure S10e, f). Noteworthy, a legible Pt-free MOF shell (ca. 22 nm) was also obtained. Analysis of the cores by HRTEM indicated that the inter planar spacing of the particle lattice was 0.185 nm, corresponding to the (111) lattice spacing of face-centered cubic Pt (Figure S10g). HAADF-STEM image (Figure S8h) and EDX elemental mapping (Figure S10i) further demonstrated that Pt, C, O and Zr were homogenously distributed on the core-shell structure. Furthermore, the characteristic diffraction peaks were in good agreement with those of pristine UiO-66 (Figure S11). These results demonstrated that the proposed surfactant-free controlled encapsulation strategy could also be achieved by controlling the formation rate of MOFs.

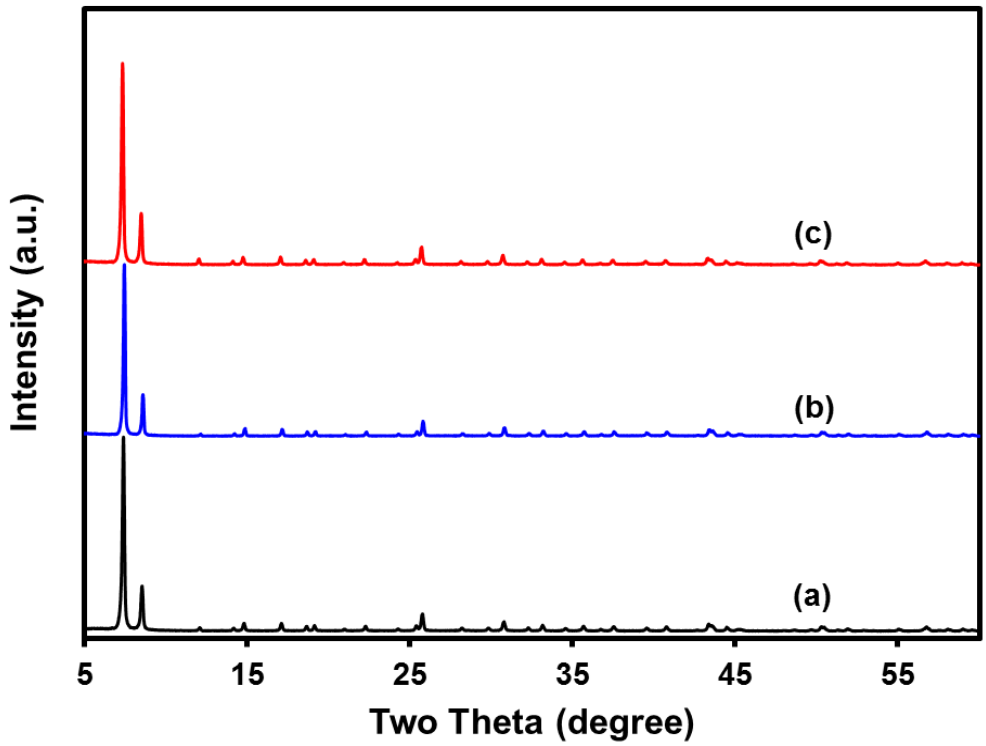

Figure S11. Powder XRD patterns of Pt@UiO-66 nanocomposites prepared with 0 (a), 60 (b), and 90 (c) equivalents of acetic acid.

References

[1] J. H. Cavka, S. Jakobsen, U. Olsbye, N. Guillou, C. Lamberti, S. Bordiga, K. P. Lillerud, *J. Am. Chem. Soc.* **2008**, *130*, 13850.

[2] a) Y. Pan, B. Yuan, Y. Li, D. He, *Chem. Commun.* **2010**, *46*, 2280; b) J. Lin, B. Qiao, J. Liu, Y. Huang, A. Wang, L. Li, W. Zhang, L. F. Allard, X. Wang, T. Zhang, *Angew. Chem. Int. Ed.* **2012**, *51*, 2920.

[3] a) A. Schaate, P. Roy, A. Godt, J. Lippke, F. Waltz, M. Wiebcke, P. Behrens, *Chem. Eur. J.* **2011**, *17*, 6643; b) H. Wu, Y. S. Chua, V. Krungleviciute, M. Tyagi, P. Chen, T. Yildirim, W. Zhou, *J. Am. Chem. Soc.* **2013**, *135*, 10525; c) T. Tsuruoka, S. Furukawa, Y. Takashima, K. Yoshida, S. Isoda, S. Kitagawa, *Angew. Chem. Int. Ed.* **2009**, *48*, 4739; *Angew. Chem.* **2009**, *121*, 4833; d) E. D. Bloch, D. Britt, C. Lee, C. J. Doonan, F. J. Uribe-Romo, H. Furukawa, J. R. Long, O. M. Yaghi, *J. Am. Chem. Soc.* **2010**, *132*, 14382.